Plasmonic Nanoparticles

DOI: 10.1002/anie.201102151

# Single Gold Nanoparticles as Real-Time Optical Probes for the Detection of NADH-Dependent Intracellular Metabolic Enzymatic Pathways**

*Lei Zhang, Yang Li, Da-Wei Li, Chao Jing, Xiaoyuan Chen, Min Lv, Qing Huang, Yi-Tao Long,* and Itamar Willner*

Plasmonics, is an emerging subfield of nanophontonics, and it attracts increasing attention because of its potential applications in controlling and manipulating light at nanoscale dimensions.[1] The advent of dark-field microscopy (DFM) has enabled the study of plasmonic nanoparticles, especially the coinage metals and the effects of their size, shape, composition as well as the local environment, which further facilitate its use in biological-labeling and detection.[2] DFM provides a direct means to probe chemical reactions, real-time optical sensing with high sensitivity, and the in vivo imaging of cancer cells. Recently, redox reactions were directly monitored on single gold nanocrystals using DFM.[3] Actually, every individual nanoparticle (NP) in the assembly could potentially act as an independent probe. Single-nanoparticle sensing platforms offer advantages since they are readily implemented in multiplex detection.[1a,4] Single nanoparticle probes offer improved absolute detection limits and also enable higher spatial resolution. Single nanoparticles have promising applications for measurements in vitro and in vivo events that are non-reachable by fixed solid array.[5] However, the use of plasmonic nanoparticles for the detection of biomolecules or biological processes is still scarce.[6]

Nicotinamide adenine dinucleotide/reduced nicotinamide adenine dinucleotide ($NAD^+$/NADH) plays an important role as cofactor in numerous biocatalyzed processes, including energy metabolism, mitochondrial responses, immunological functions, aging and cell death.[7] The catalytic deposition of copper on gold nanoparticles (AuNPs) by the NADH cofactor has been applied for the optical and electrochemical detection of NADH and $NAD^+$-dependent biocatalytic processes.[8] Herein, we describe a novel method to detect enzymatic activity at the single particle level inside and outside cells by DFM. To our knowledge, it is the first time to monitor the intracellular metabolism and the effect of anticancer drugs on the cell metabolism using copper growth on the AuNP probes.

To investigate the application of single Au@Cu nanoparticles for nano-sensing, the plasmon resonance Rayleigh scattering (PRRS) spectra $\lambda_{max}$ of a single particle was used to probe the gold-catalyzed reduction of $Cu^{2+}$ ions on AuNPs by NADH or by $NAD^+$-cofactor-dependent enzyme/substrate system that generates NADH (Scheme 1). Compared with the scattering spectra in the absence of NADH, the scattering spectra acquired with NADH exhibit a distinct peak shift

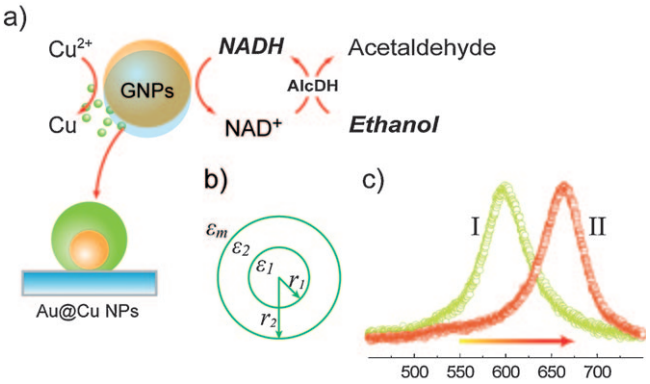


***Scheme 1.*** a) Enlargement of AuNP seeds by the AuNPs-catalyzed deposition of a Cu shell (green), when treated with a $Cu^{2+}$ source in the presence of the reducing agent NADH. The NADH can be generated from $NAD^+$ by oxidation of an alcohol catalyzed by an enzyme (alcohol dehydrogenase) See text for details. b) The parameters controlling the Rayleigh scattering spectra of Au@Cu core–shell NPs, where $\varepsilon_1$ and $\varepsilon_2$ correspond to the real dielectric constant of the Au core and Cu shell, respectively, and $\varepsilon_m$ is the dielectric constant of the adjacent medium (i.e., solvent); $r_1$ and $r_2$ correspond to the radius of AuNP before and after coating with Cu shell. c) Scattering spectra before (I) and red-shift after (II) the single Au@Cu core–shell NPs were formed.

[*] L. Zhang,[+] Dr. Y. Li,[+] Dr. D.-W. Li, C. Jing, Prof. Y.-T. Long
Shanghai Key Laboratory of Functional Materials Chemistry
East China University of Science and Technology
Shanghai, 200237 (P. R. China)
Fax: (+86) 21-6425-0032
E-mail: ytlong@ecust.edu.cn

Prof. X. Chen
Laboratory of Molecular Imaging and Nanomedicine
National Institute of Biomedical Imaging and Bioengineering
National Institutes of Health, Bethesda, MD 20892 (USA)

M. Lv, Prof. Q. Huang
Laboratory of Physical Biology
Shanghai Institute of Applied Physics
Chinese Academy of Sciences, Shanghai, 201800 (P. R. China)

Prof. I. Willner
Institute of Chemistry, The Hebrew University of Jerusalem
Jerusalem, 91904 (Israel)

[+] These authors contributed equally to this work.

[**] This research is supported by the Major Research Plan of National Natural Science Foundation of China (91027035), Key Program of National Natural Science of China (20933007), and Shanghai Pujiang Program Grant of China (09PJ1403300).

Supporting information for this article is available on the WWW under http://dx.doi.org/10.1002/anie.201102151.

toward longer wavelengths (Scheme 1c), consistent with the occurrence of the resonance coupling within the Au@Cu core–shell nanostructure. The PRRS spectra peak shift ($\Delta\lambda_{max}$) increased rapidly at the beginning of the deposition of the Cu aggregates and then the shifts leveled off to a saturation value. These shifts of the AuNPs PRRS spectra provided the basis for the design of optical nanosensor based on a plasmonic single AuNP.

The sensitivity of the AuNPs PRRS spectra $\lambda_{max}$ to changes in the local dielectric environment is determined by differences in size[9] (see Figure S2 in the Supporting Information). Although single nanoparticles enable highly sensitive detection with clear spatial resolution, the nanoparticle size must be selected with care to ensure sufficient signal intensity for $\Delta\lambda_{max}$ assays. The AuNPs do not show any shift in $CuCl_2$ solution. Nonetheless, 2 h after the injection of NADH to the AuNPs/$CuCl_2$ solution, the scattering spectra of all AuNPs immobilized on the microscope slide were red-shifted by varying degrees. The PRRS spectra of the AuNPs before and after formation of the Au@Cu core–shell nanostructures match well with the diameters of the nanoparticles (see Figure S3 in the Supporting Information). In the presence of 20 μM $CuCl_2$ and 30 nM NADH, the NADH-catalytic growing process of copper shell on a single AuNP with the initial scattering peak around 575 nm was observed (Figure 1a). The scattering peak ($\lambda_{max}$) red shifted to longer wavelength continuously. Time-dependent $\Delta\lambda_{max}$ changes of three selected AuNPs with different sizes, on treatment, are shown in Figure 1c. The $\Delta\lambda_{max}$ shifts of up to 30 nm were observed upon the formation of the Au@Cu nanostructure after 2 h. Statistical analysis of the scattering spectra of a number of AuNPs revealed that the original AuNP peak ($\lambda_{max}$) in the scattering spectrum located at around 590 nm (the corresponding diameter of the AuNPs is about 80 nm) was significantly shifted after the formation of copper shell structure (Figure 1d). One single AuNP with an initial scattering peak around 600 nm was selected from the sample (Figure 1b) as a probe for different concentrations of NADH. $\Delta\lambda_{max}$ of this nanoparticle increases linearly with the increasing concentration of NADH (Figure 1e), which indicates a higher content of Cu deposition on the AuNPs surface.

The resulting scattering spectra of the NADH-generated Cu nanoshells are in good agreement with the Mie scattering theory and exhibit this behavior for a variety of shell thicknesses.[10] Based on the computational model shown in Scheme 1b, the PRRS spectra $\Delta\lambda_{max}$ of a single spherical metal nanoparticle is governed by Equations (1) and (2) (See Supporting Information), where $\varepsilon_1$ and $\varepsilon_2$ correspond to the dielectric constant of gold core and Cu shell respectively, $\varepsilon_m$ is the dielectric constant of the adjacent medium (i.e., solvent), $V_1$ and $V_2$ (the volume of AuNP before and after coating with Cu shell) can be calculated by its radius $r_1$ and $r_2$, the $c_{NADH}$ correspond to the concentration of NADH.

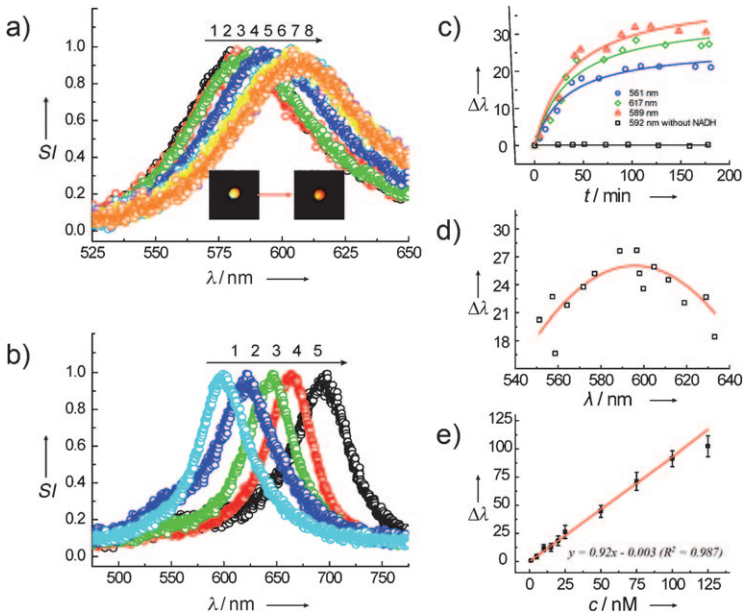


***Figure 1.*** a) Representative time-dependent single AuNP scattering spectra upon treating the AuNPs with $CuCl_2$ 20 μM and NADH 30 nM, showing that the $\lambda_{max}$ of the PRRS spectra are red shifted, spectra 1–8: 0, 5, 13, 24, 41, 59, 87, 131 min. The insets shows the color image of a typical AuNP before and after being covered by the Cu shell, demonstrating the color transition from yellow to red. b) The PRRS spectra of Au@Cu core–shell nanoparticles upon interaction with different concentrations of NADH for a fixed time interval of 2 h, spectra 1–5: 0, 25, 50, 75, 100 nM of NADH. c) Time-dependent $\Delta\lambda_{max}$ changes of three different sized AuNPs with $\lambda_{max}$ values of 561 nm (○), 589 nm (△) and 617 nm (◇) upon treatment with $CuCl_2$/NADH. d) Distribution curve corresponding to the $\Delta\lambda_{max}$ values of a collection of different AuNPs treated with $CuCl_2$/NADH for 2 h. The red line is the Gaussian fit of the experimental data. e) Calibration plot corresponding to the $\Delta\lambda_{max}$ shifts of the PRRS spectra at different concentrations $c$ of NADH for a single AuNP. (The scattering intensities (*SI*) of the all the spectra have been normalized.)

$$\Delta\lambda_{max} = \frac{\Delta V}{V_1 + 2\Delta V + \frac{\Delta V^2}{V_1}} \Big/ \left[ d\frac{(2\varepsilon_2 - 2\varepsilon_m)(\varepsilon_1 - \varepsilon_2)}{(\varepsilon_2 + \varepsilon_m)(\varepsilon_1 + 2\varepsilon_m)} \Big/ d\lambda \right] \quad (1)$$

$$\Delta V = V_2 - V_1 = k_1 c_{NADH} + b \quad (2)$$

That is, $\Delta\lambda_{max}$ is dependent on $\Delta V$ ($c_{NADH}$) and $V_1$. When $V_1$ keeps constant, $\Delta\lambda_{max}$ is proportional to $\Delta V$ ($c_{NADH}$) in a certain concentration range of NADH. While under a fixed NADH concentration $\Delta\lambda_{max}$ reaches maximum and then decreases with the increasing of $V_1$. The result fits well with Equation (1) realizing that the diameter of AuNPs increases from 50 nm to 110 nm, and further proves the maximum response was obtained for approximately 80 nm AuNPs (Figure 1d).

To determine the sensitivity of this method, and to evaluate the applicability of the system for sensing, changes in PRRS spectra ($\Delta\lambda_{max}$) were determined at different NADH concentrations in the range of 1–100 nM. As shown in Figure 1b,e, the peak of single AuNP nanoprobe's PRRS spectra, $\lambda_{max}$, shifts to a longer wavelength as the concentrations of NADH increases. And a linear relation between the $\Delta\lambda_{max}$ and the NADH concentration is observed.

  

The successful analysis of NADH by the $\lambda_{max}$ shift in the PRRS spectra suggested that the system might be used to follow biocatalyzed transformations that involve $NAD^+$-dependent enzymes. Accordingly, the $NAD^+$-dependent alcohol dehydrogenase (AlcDH) was treated with a constant concentration of $NAD^+$ and ethanol, leading to the formation of the reduced cofactor NADH (Scheme 1a and Figure 2c). The resulting NADH-containing solution was heated to 100 °C to stop the enzymatic reaction and then transferred to a developing solution containing $Cu^{2+}$ ions on the AuNP-functionalized microscopy slides. Similar to the results of NADH-catalyzed reaction, there is no wavelength shift without of the NADH-containing solution, but 2 h after the addition of the NADH-containing solution, the scattering spectra of all the AuNPs were red-shifted to various degrees (Figure 2d). The AuNPs with scattering peak located around 594 nm gave the maximum red shift (see Figure S4 in the Supporting Information). The $\Delta\lambda_{max}$ of AuNPs increased upon the further injection of the NADH-containing solution. Control experiments indicated that the deposition of Cu did not proceed in the developing solution if any of the components ethanol, AlcDH, or $NAD^+$ were excluded from the parent solution (Figure 2d). These results clearly indicate that NADH, which acts as the reducing agent, is essential to affect the deposition of Cu in the developing solution. The electrochemical stripping analysis of Cu by the Au@Cu core–shell NPs modified ITO plates was performed after growth for 3 h in the developing solution. Chronocoulometric transients were observed upon stripping off the Cu deposited on the AuNPs by the NADH biocatalytic system (see Figure S5, Supporting Information). As expected, the PRRS spectra of the AuNPs ensemble were blue-shifted to almost the original position after the stripping out of Cu. The thickness of shell on the Au@Cu nanoparticles was calculated to be about 25 ± 4 nm when the concentration of NADH was 25 nM. These results coincided well with the SEM results (23 ± 8 nm), which clearly indicate that the presence of NADH, acting as the reducing agent, is essential to affect the deposition of Cu in the developing solution.

The balance between $NAD^+$/NADH reflects both the metabolic activities and the health of cells.[11] The fact that intracellular metabolism of cancer cells is regulated by anticancer agents, such as taxol, suggests that the NADH-dependent gold-catalyzed growth of Au@Cu core–shell NPs could be used as optical probes for anticancer drugs, and thus, may provide a method for the screening of such drugs. Indeed, there are reports of the inhibition of intracellular metabolism of A549 cancer cells and HeLa cell by taxol.[12] AuNPs, as label-free probes, could penetrate the membrane, and dispersed around the nuclei and lysosomes. Figure 3 shows the DFM image changes reflecting the dynamic behavior of the gold-catalyzed reductive deposition of Cu on the AuNPs in individual HeLa cells. Based on the previous experiments, the changes of the scattering spectra of the AuNPs probes were recorded in HeLa cells, and the peak continually shifted to longer wavelengths. In turn, taxol suppresses the metabolism in the cancer cells, thus leading to inefficient yields of NADH and lower PRRS spectra $\lambda_{max}$ shifts for the AuNPs probes (Figure 3i-1 to i-4 and l-1 to l-4). The formation of the Au@Cu core–shell nanoparticles in the HeLa cancer cells was confirmed by HRTEM measurements (Figure 3m,n). After the disruption of the HeLa cells by the osmotic shock method, the HRTEM image of the nanoparticles indicates an Au core structure with the characteristic Au crystalline spacing of 0.238 nm that is coated with a Cu layer exhibiting a thickness of approximately 4 ± 1.5 nm. These results suggest that the plasmonic AuNP probes and $Cu^{2+}$ ions may be used for screening anticancer drugs that affect the intracellular metabolism.

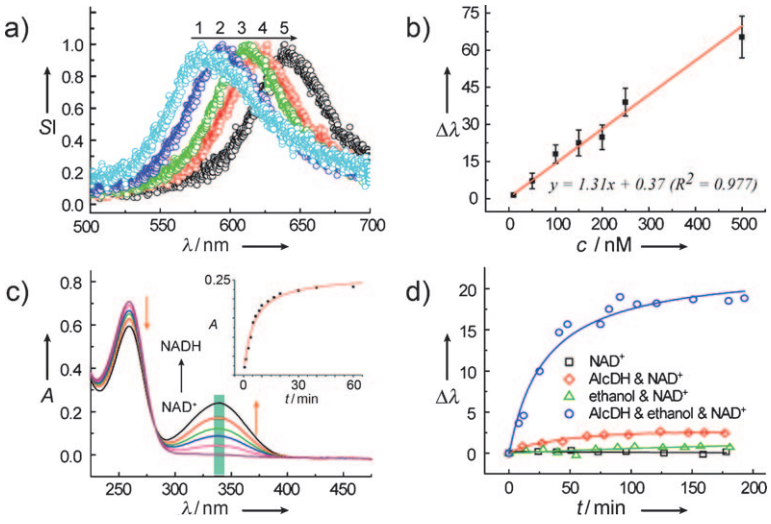


***Figure 2.*** a) Representative scattering spectra of a typical single AuNP in developing solution containing a varying concentration of mixture (spectra 1–5: 0, 100, 200, 250, 500 nM of ethanol; after a fixed reaction time of 30 min, medium: 1 mM $NAD^+$, 0.1 mg mL$^{-1}$ AlcDH, and 20 μM $CuCl_2$). b) Calibration plot corresponding to the PRRS spectra $\Delta\lambda_{max}$ shift with developing solution containing different concentrations of ethanol. c) Real-time UV/Vis spectra of the mixture of $NAD^+$ (1 mM), ethanol (1 μM) and AlcDH (0.1 mg mL$^{-1}$) at different times; Inset: the relationship between intensity (340 nm; green bar in the main spectrum) and time. d) The plots of scattering spectra $\Delta\lambda_{max}$ versus time for AuNPs under different conditions.

In conclusion, we introduced a novel method based on dark-field microscopy to detect the NADH cofactor or to follow $NAD^+$-dependent biocatalyzed transformations. The method involves the NADH-mediated reduction of $Cu^{2+}$ onto AuNPs forming Au@Cu core–shell nanoparticles. The PRRS spectra of the Au@Cu nanoparticles are red-shifted as the concentration of NADH increases or as the concentration of NADH, generated in the presence of $NAD^+$ and the cofactor-dependent enzyme, increases. The fact the each individual AuNP acts as a probe for the local quantified detection of NADH enables the miniaturization of the sensor system, and the use of microscale droplets as analysis volumes. Furthermore, our studies demonstrated the ability to use DFM and scattering spectra to monitor in vitro the metabolism in HeLa cancer cells, and particularly to probe the effect of an anticancer drug (taxol) on the cell metabolism. We anticipate that these discoveries add important tools for the imaging of cells, mapping the distribution of NADH in cells, to follow in-vitro intracellular

  

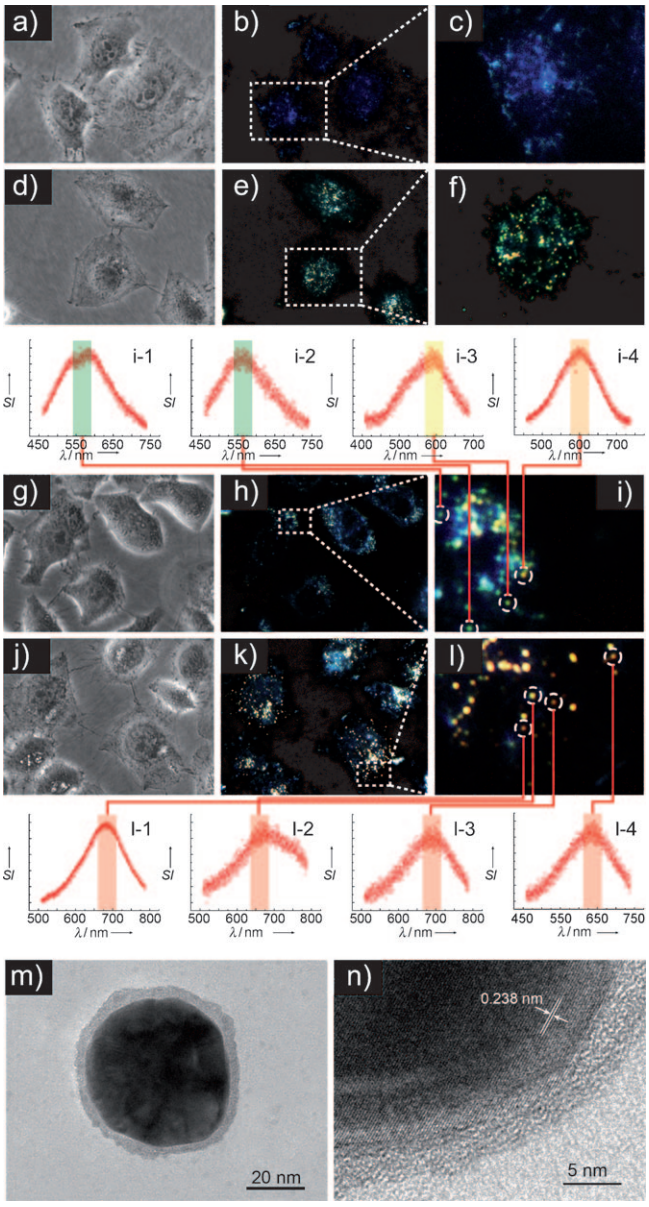


***Figure 3.*** a) Bright-field images of HeLa cell. b) DFM images of corresponding HeLa cell in (a). c) the detail view of HeLa cell DFM images (b). d) Bright-field images of HeLa cell after 24 h incubation with AuNPs. e) DFM images of corresponding HeLa cell in (d). f) the detail view of HeLa cell containing AuNPs DFM images (e). g) Bright-field images of HeLa cell containing AuNPs with treatment by taxol (10 μM) and then incubation in TBS containing 50 μM $CuCl_2$ for 3 h. h) DFM images of corresponding HeLa cell in (g). i) the detail view of HeLa cell DFM images (h), i-1 to i-4: Corresponding scattering spectra of different AuNPs in living HeLa cell. j) Bright-field images of HeLa cell containing AuNPs without treatment by taxol and then incubation in TBS containing 50 μM $CuCl_2$ for 3 h. k) DFM images of corresponding HeLa cell in (j). l) the detail view of HeLa cell DFM images (k), l-1 to l-4: Corresponding scattering spectra of different Au@Cu core–shell NPs in living HeLa cell (the color bar in the scattering spectra indicate the wavelength of the maximum scattering intensity, and reflect the resulting color). m) HRTEM image of a single Au@Cu core–shell nanoparticle. n) Enlargement image of the Au@Cu core–shell nanoparticle.

metabolic pathways, and to screen drugs affecting cell metabolism. Accordingly, future efforts will be directed to characterize other biocatalytic processes using single plasmonic nanoparticles.

## *Experimental Section*

Seed AuNPs of 13 nm diameter were synthesized using citrate to reduce $Au^{3+}$ following a literature procedure.[13] These particles were then used as seed particles for the synthesis of gold particles larger than 20 nm by $NH_2OH{\cdot}HCl$ reduce growth methods.[14] Modification procedure, analysis methods, cell culture, single nanoparticle DFM imaging, and scattering spectroscopy collection were performed as described in the Supporting Information.

Received: March 28, 2011
Published online: June 9, 2011

**Keywords:** gold nanoparticles · metabolic pathways · NADH · plasmon resonance Rayleigh scattering

[1] a) J. N. Anker, W. P. Hall, O. Lyandres, N. C. Shah, J. Zhao, R. P. Van Duyne, *Nat. Mater.* **2008**, *7*, 442; b) S. Lal, S. Link, N. J. Halas, *Nat. Photonics* **2007**, *1*, 641; c) S. Eustis, M. A. El-Sayed, *Chem. Soc. Rev.* **2006**, *35*, 209.
[2] X. H. Huang, P. K. Jain, I. H. El-Sayed, M. A. El-Sayed, *Nanomedicine* **2007**, *2*, 681.
[3] C. Novo, A. M. Funston, P. Mulvaney, *Nat. Nanotechnol.* **2008**, *3*, 598.
[4] Y. Choi, Y. Park, T. Kang, L. P. Lee, *Nat. Nanotechnol.* **2009**, *4*, 742.
[5] a) K. Lee, P. Nallathamby, L. Browning, C. Osgood, X. Xu, *ACS Nano* **2007**, *1*, 133; b) X. Xu, W. Brownlow, S. Kyriacou, Q. Wan, J. Viola, *Biochemistry* **2004**, *43*, 10400; c) D. Lasne, G. Blab, S. Berciaud, M. Heine, L. Groc, D. Choquet, L. Cognet, B. Lounis, *Biophys. J.* **2006**, *91*, 4598; d) D. Shotton, *J. Cell Sci.* **1989**, *94*, 48; e) J. Aaron, N. Nitin, K. Travis, S. Kumar, T. Collier, S. Y. Park, M. Jose-Yacaman, L. Coghlan, M. Follen, R. Richards-Kortum, K. Sokolov, *J. Biomed. Opt.* **2007**, *12*, 034007; f) G. L. Liu, Y.-T. Long, Y. Choi, T. Kang, L. P. Lee, *Nat. Methods* **2007**, *4*, 1015; g) G. L. Liu, Y. D. Yin, S. Kunchakarra, B. Mukherjee, D. Gerion, S. D. Jett, D. G. Bear, J. W. Gray, A. P. Alivisatos, L. P. Lee, F. Q. F. Chen, *Nat. Nanotechnol.* **2006**, *1*, 47.
[6] G. Raschke, S. Kowarik, T. Franzl, C. Sönnichsen, T. A. Klar, J. Feldmann, A. Nichtl, K. Kürzinger, *Nano Lett.* **2003**, *3*, 935.
[7] W. H. Ying, *Antioxid. Redox Signaling* **2008**, *10*, 179.
[8] a) B. Shlyahovsky, E. Katz, Y. Xiao, V. Pavlov, I. Willner, *Small* **2005**, *1*, 213; b) Y. Xiao, V. Pavlov, S. Levine, T. Niazov, G. Markovitch, I. Willner, *Angew. Chem.* **2004**, *116*, 4619; *Angew. Chem. Int. Ed.* **2004**, *43*, 4519.
[9] a) A. D. McFarland, R. P. Van Duyne, *Nano Lett.* **2003**, *3*, 1057; b) S.-K. Eah, H. M. Jaeger, N. F. Scherer, G. P. Wiederrecht, X.-M. Lin, *Appl. Phys. Lett.* **2005**, *86*, 031902.
[10] H. Wang, F. Tam, N. K. Grady, N. J. Halas, *J. Phys. Chem. B* **2005**, *109*, 18218.
[11] F. Q. Schafer, G. R. Buettner, *Free Radical Biol. Med.* **2001**, *30*, 1191.
[12] a) R. Freeman, R. Gill, I. Shweky, M. Kotler, U. Banin, I. Willner, *Angew. Chem.* **2009**, *121*, 315; *Angew. Chem. Int. Ed.* **2009**, *48*, 309; b) J. Park, H. Y. Lee, M. H. Cho, S. B. Park, *Angew. Chem.* **2007**, *119*, 2064; *Angew. Chem. Int. Ed.* **2007**, *46*, 2018.
[13] K. C. Grabar, R. G. Freeman, M. B. Hommer, M. J. Natan, *Anal. Chem.* **1995**, *67*, 735.
[14] K. R. Brown, D. G. Walter, M. J. Natan, *Chem. Mater.* **1999**, *12*, 306.

  